

Ab Initio Structure and Vibrational Frequencies of $(\text{CF}_3\text{SO}_2)_2\text{N}^-\text{Li}^+$ Ion Pairs

Shridhar P. Gejji,* C. H. Suresh,† K. Babu, and Shridhar R. Gadre

Department of Chemistry, University of Pune, Pune 411 007, India

Received: November 18, 1998; In Final Form: May 11, 1999

The cation coordination of the bis(trifluoromethanesulfone)imide (TFSI) anion $(\text{CF}_3\text{SO}_2)_2\text{N}^-$ has been studied using the molecular electrostatic potential (MESP) topography as a tool. The critical points of MESP are employed for searching the cation binding sites of the anion. Subsequent ab initio Hartree–Fock calculations using the 6-31G(d) basis for the Li^+TFSI^- ion pair engenders seven local minima on the potential energy surface of the complex. In the lowest energy conformer, Li^+ coordinates with two oxygens, one from each of the different SO_2 groups on the central nitrogen, with the anion having C_2 point group symmetry. Li^+TFSI^- conformers with the cation in coordination (a) with oxygen and nitrogen atoms of the anion or (b) with the two oxygens of the same SO_2 group as well as (c) with the oxygen and one of the fluorines at the CF_3 end, typically 48–114 kJ mol^{-1} higher in energy than the lowest minimum, have also been obtained. The SNS bond angle in the free anion as well as that in the Li^+TFSI^- ion pair turns out to be in the range 126° – 132° , which agrees well with the X-ray data on the crystal hydrate structure for the HTFSI. A comparison of the vibrational spectra of the free TFSI anion and the Li^+TFSI^- ion pair conformers reveals that the S–N stretching vibration at 815 cm^{-1} can be used as a probe to distinguish the different ion pair conformers. A near doublet at the 703 cm^{-1} in the C_2 symmetry of the TFSI anion on coordination shows a separation of 7 – 60 cm^{-1} in the ion pair.

1. Introduction

Lithium trifluoromethanesulfonimide $\text{Li}(\text{CF}_3\text{SO}_2)_2\text{N}$ (Li^+TFSI^-) was introduced by Armand et al.¹ as a plasticizing salt in polymer electrolytes and suggested to have great technological importance. It has been demonstrated that $\text{Li}(\text{CF}_3\text{SO}_2)_2\text{N}$ acts as a good plasticizer in poly(ethylene oxide) (PEO) based electrolytes, producing a high-conductivity material with a wide electrochemical stability window.² These properties render the polymer materials suitable for solid-state batteries. The crystal structure of poly(ethylene oxide)– $\text{Li}(\text{CF}_3\text{SO}_2)_2\text{N}$ from the powder diffraction have been reported by Bruce et al.³ using a Monte Carlo approach. Ion–polymer and the ion–ion interactions of Li^+TFSI^- complexed with poly(propylene oxide) (PPO) have been investigated⁴ via nuclear magnetic resonance (NMR), differential scanning calorimetry (DSC), and electrical impedance techniques. Vallee et al.⁵ have compared the phase transitions in mixtures of PEO and Li^+TFSI^- with those of the PEO– LiCF_3SO_3 and PEO– LiClO_4 systems. Li^+TFSI^- is found to be more soluble in PEO than LiCF_3SO_3 and LiClO_4 . From the NMR experiments, Tegenfeldt et al.⁶ have found the diffusion behavior of the anions in the low molecular weight polymer electrolytes comprising LiCF_3SO_3 and $\text{Li}(\text{CF}_3\text{SO}_2)_2\text{N}$ in poly(ethylene glycol) (PEG) is similar. Lindgren et al.⁷ have measured the infrared spectra of alkaline earth metal (M) coordinated TFSI anion in the poly(ethylene oxide) (PEO), and the formation of the $\text{M}^{2+}(\text{TFSI}^-)_2$ ion pairs has been discussed on the basis of frequency shifts of the characteristics S–N stretching vibrations. The possibility of the formation of the cation–TFSI[−] ion pairs, which is an important factor underlying these ion transport phenomenon, thus remains an open question to date. FTIR transmission spectra of the films of the PEO–

LiTFSI mixtures have been used in constructing the phase diagram of these systems.⁸ Rey et al.⁹ have investigated the conformational changes of the PEO in the $\text{P}(\text{EO})_n$ – LiTFSI complexes and presented a tentative assignment of characteristic vibrations of the TFSI anion. Recently, the $\text{Li}^+(\text{CF}_3\text{SO}_2)_2\text{N}^-$ ion pairs have been studied with the ab initio quantum chemical methods¹⁰ using the 3-21+G basis. These calculations yield the SNS angle to be 156° . On the other hand, the SNS angle in the salt hydrate structure of the HTFSI determined from the X-ray experiments¹¹ range from 125° to 128° . Johansson et al.¹² have recently calculated the potential energy surface through the S–N bond rotations of the free TFSI anion employing the larger 6-31G(d) and 6-31+G(d) basis sets. The flexible nature of the free anion leads to two local minima with the C_2 and C_1 point group symmetries (These are denoted as **A1** and **A2**, respectively, cf. Figure 1). The **A2** conformer which is merely 2.3 kJ mol^{-1} higher in energy than **A1**, was not reported by Arnaud et al.¹⁰ Thus, with the extension of the basis to 6-31G(d) for the **A1** conformer of the anion, the SNS angle turns out to be nearly 128° , which is in good agreement with that for the anion in the salt hydrate HTFSI.¹¹ The SNS angle for the conformer with no symmetry (**A2**) turns out to be 126° . Further, the extension of the basis set by adding the diffuse functions on all the atoms of the free anion in the 6-31G(d) basis, that is, the 6-31+G(d) basis, produces a change of less than 1° for the SNS angle in both the anionic conformers. Ab initio calculated geometries and the vibrational spectra of the free HTFSI molecule with the C_2 point group symmetry have recently been reported in the literature.¹³ It should be noted that the **A2** conformer of the free TFSI anion renders additional possibilities of binding for the coordinating cation. Thus, a large deviation of the SNS angle, from 156° to 126 – 128° , and a location of the **A2** conformer for the free anion, merely 2 kJ mol^{-1} higher in energy than **A1**, necessitates the reassessment of the structure

* Present address: Graduate school of Human Informatics, Nagoya University, Chikusaku, Nagoya 464-8601, Japan.

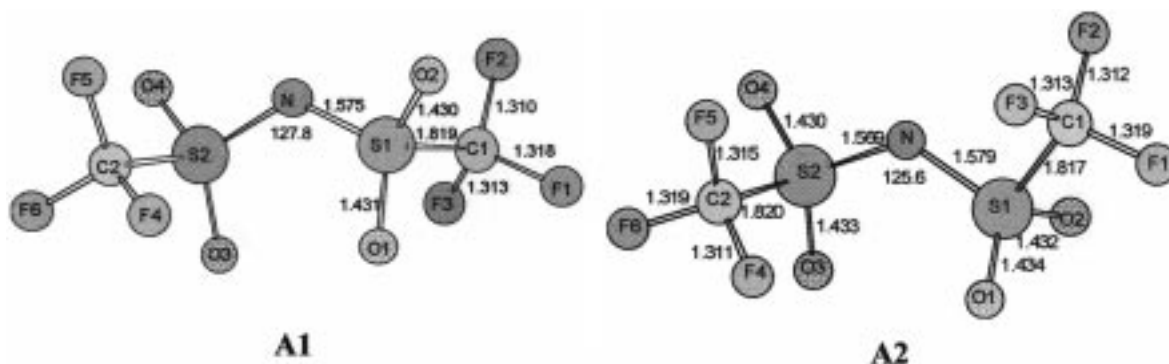


Figure 1. Conformers of the free TFSI anion with C_2 (**A1**) and C_1 (**A2**) point group symmetries.

and energetics of the LiTFSI ion pairs reported by Arnaud and co-workers. It has been pointed out by Arnaud et al.¹¹ that the affinity of Li toward the anion is mainly due to the electrostatic effects and contributions from the charge-transfer interactions are less important. This is interesting since the scalar fields of molecular electrostatic potential (MESP), known to be successful in studying a wide variety of intermolecular interactions,^{14–22} may then be used to gain deeper insights in the formation of the cation–TFSI ion pairs. In view of this, we herewith focus on the energies of the Li⁺TFSI⁻ ion pair conformers, with the MESP topography of the anion as a tool. It has been demonstrated here that the ion pair formation is guided by the MESP topography of the anion solely. Although the effects due to geometry relaxation play a significant role in this case, the present model provides a systematic approach to study the conformational energies of the Li⁺TFSI⁻ ion pairs. The computational method has been outlined in section 2, which is followed by results and discussion in section 3. Concluding remarks have been summarized in section 4.

2. Computational Method

Ab initio Hartree–Fock (HF) SCF MO calculations have been performed for the free anion using the GAUSSIAN 94 program.²³ The internally stored 6-31G(d) basis was used. The MESP $V(\mathbf{r})$ at a point r due to a molecular system with nuclear charges $\{Z_A\}$ located at $\{\mathbf{R}_A\}$ and the electron density $\rho(\mathbf{r})$ is given by

$$V(\mathbf{r}) = \sum_A^N \frac{Z_A}{|\mathbf{r} - \mathbf{R}_A|} - \int \frac{\rho(\mathbf{r}') d^3\mathbf{r}'}{|\mathbf{r} - \mathbf{r}'|} \quad (1)$$

where N is the total number of nuclei in the molecule. The first term in eq 1 refers to the bare nuclear potential and the second to the electronic contribution. The topography of MESP is mapped by examining the eigenvalues of the Hessian matrix at the point where the gradient of $V(\mathbf{r})$ vanishes. The MESP was calculated and the MESP critical points (CPs) were located using a fortran code UNIPROP.²⁴ Fortran program UNIVIS²⁴ was used for visualization of the MESP topography of the anionic conformers. The MESP CPs can be characterized¹⁵ in terms of an ordered pair (rank, signature). These CPs can be grouped into three sets, viz., (3, +3), (3, +1), and (3, -1). The (3, +3) set corresponds to the set of MESP minima, and the remaining ones represent the saddle points. These CPs have been employed as potential cation binding sites. A cation is placed near the CP, and its optimum position is determined (without disturbing the geometry of the anion) by minimization of the electrostatic interaction energy $E_{\text{int}}^{\text{dock}}$

$$E_{\text{int}}^{\text{dock}} = \int V_A(\mathbf{r})\rho_c(\mathbf{r}) d^3r \quad (2)$$

Here, $V_A(\mathbf{r})$ refers to the electrostatic potential of the anion and $\rho_c(\mathbf{r})$ denotes the charge density of the cation at that site. The coalescence of the anion and cation is prevented by limiting the distance of closest approach by defining the boundary surface for the ions. Pauling ionic radius is used for the cation, and the CP distribution defines the anionic boundary. In the present work, the ion pair geometries derived from the minimization of interaction energy given by eq 2 will be referred to as “docked geometries”. Only the symmetry-unrelated CPs are considered for the electrostatic docking in case of the **A1** conformer. The docked ion pair geometries thus derived were subjected to the optimization in the HF calculations with the GAUSSIAN 94 program subsequently using the analytical gradient relaxation method. Local minima were confirmed through the vibrational frequency calculations.

3. Results and Discussion

a. TFSI Anion: Geometry and MESP Topography. Two conformations of TFSI anion, with C_2 and C_1 symmetries, respectively, are displayed in parts a and b of Figure 1. The important structural difference between the two conformers is in the CSSC twist angle. This angle is 174° for the **A1** conformer and 70° for the **A2** conformer. The SNS bond angle is close to the experimental value (125°–128°) reported¹¹ for the HTFSI molecule. The C–F bond lengths in the **A1** conformer of the anion, however, are nearly 0.05 Å longer than the corresponding ones obtained from the X-ray data on the HTFSI. The shortening of the C–F bond lengths in the experiments may partly be attributed to a large disorder in the HTFSI crystal, manifested in the large mean-square amplitudes for the two fluorine atoms involved in these bonds¹³. The two conformers differ in energy by only 2.3 kJ.

Anions in general possess a rich MESP topography,^{14,21,22} which is very clear in this case too. The MESP topography shows 38 negative valued CPs for the **A1** and 39 for **A2** conformer of the anion, characterized in terms of rank and signature as pointed out in the preceding section. The number of (3, +3), (3, +1), and (3, -1) CPs for the **A1** and **A2** conformers are (9, 19, 10) and (6, 18, 15), respectively, with the MESP values ranging from -286 to -543 kJ mol⁻¹. The MESP isosurfaces of -507 kJ mol⁻¹, along with the corresponding CPs, in the **A1** as well as that in the **A2** conformers of the anion are displayed in Figure 2. These CPs represent the probable cation binding sites of the free anion. Although the MESP value at the CP of the nitrogen atom (-563 kJ mol⁻¹) of **A1** conformer is more negative than that for oxygen (-558 kJ mol⁻¹), the volume enclosed by the above-specified MESP

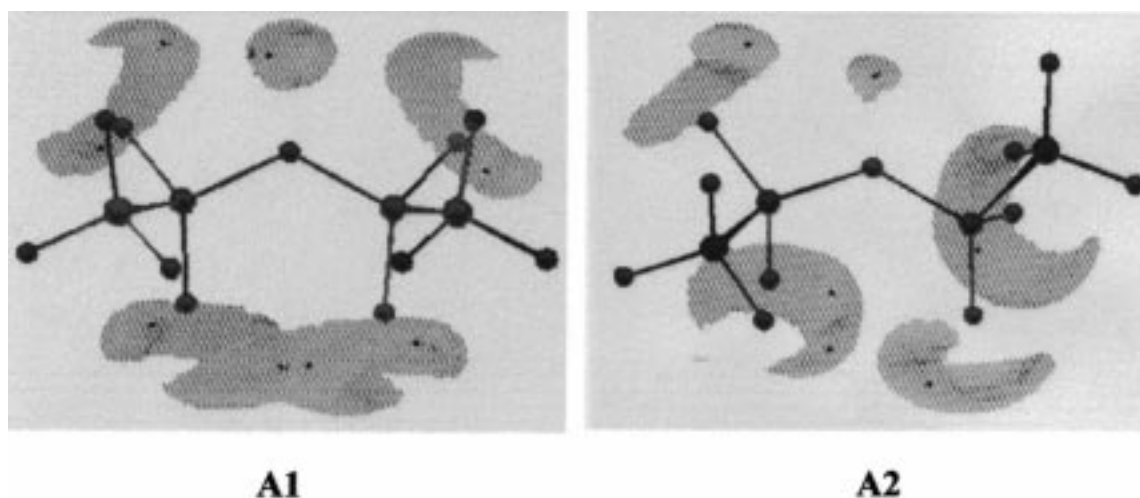


Figure 2. MESP isosurface of -507 kJ mol^{-1} for the TFSI anion with C_2 (**A1**) and C_1 (**A2**) point group symmetries along with the (3, +3) CPs, respectively.

TABLE 1: Net Atomic Charges in the A1 and A2 Conformers of the TFSI Anion Derived from the MESP and Mulliken Population Analysis

atom centers	A1 conformer		A2 conformer	
	MESP	Mulliken	MESP	Mulliken
N	-0.726	-0.940	-0.673	-0.952
S	1.004	1.522	1.048	1.526
S	1.009	1.522	0.946	1.539
O	-0.543	-0.669	-0.543	-0.668
O	-0.550	-0.682	-0.513	-0.688
O	-0.552	-0.682	-0.503	-0.672
O	-0.545	-0.669	-0.543	-0.685
C	0.343	0.829	0.076	0.831
C	0.350	0.829	0.250	0.836
F	-0.096	-0.337	-0.043	-0.333
F	-0.135	-0.342	-0.075	-0.345
F	-0.161	-0.351	-0.092	-0.352
F	-0.137	-0.342	-0.106	-0.342
F	-0.163	-0.351	-0.120	-0.356
F	-0.099	-0.337	-0.110	-0.339

isosurface (cf. Figure 2) seems to be more for oxygen sites than the nitrogen. This makes the cation binding more favorable toward the SO_2 end of the anion. Further, these MESP CPs can be possibly related with one or two nearest atoms. For example, a CP with MESP -543 kJ mol^{-1} is 1.27 \AA from O1 and 1.41 \AA from O3 atom. The MESP CPs below -472 kJ mol^{-1} may be associated with the oxygen atoms. It should be noted here that in the **A1** conformer each oxygen exhibits two (3, +3) CPs, whereas in the **A2** conformer only one oxygen atom shows two such CPs and the remaining ones have only one (3, +3) CP. The MESP regions surrounding the fluorines exhibit less negative (above -340 kJ mol^{-1}) saddles. It is noteworthy that no (3, +3) CPs are found in the vicinity of the CF_3 groups of the anion. The MESP-derived point charges obtained using the fortran code GRID²⁶ are also presented in Table 1 along with the corresponding Mulliken charges. It may readily be noticed that the nitrogen atom retains more negative charge than oxygens.

b. LiTFSI Ion Pair: Electrostatic Docking and Hartree-Fock Geometries. For modeling the Li^+TFSI^- ion pair, the cation is allowed to approach a CP and its optimum position is determined by minimization of the electrostatic interaction energy given in eq 2. Electrostatic docking of Li^+ with TFSI^- engenders 16 different structures for the **A2** conformer and 10 for the **A1** conformer. The interaction energies thus obtained range from -359 to -470 kJ mol^{-1} for the **A2** conformer and

-388 to -493 kJ mol^{-1} for the **A1** conformer, suggesting a slight preference of the latter for cation coordination. In addition, Li^+ prefers to bind to the oxygen atoms than to nitrogen or fluorine atoms, which can be attributed to the larger negative-valued MESP regions associated with oxygen atoms than nitrogen or fluorine atoms (cf., Figure 2). With these insights on electrostatic interactions on ion pair formation, a follow-up study at the ab initio level has been performed.

HF/6-31G(d) optimizations from all these docked ion pair geometries converged to seven different local minimum geometries **A1a-d** (anionic backbone resembling more of **A1** than **A2**) and **A2a-c** (anionic backbone resembling more of **A2** than **A1**) displayed in Figures 3 and 4. Several electrostatic docked geometries converge to the same structure on HF optimization. However, this has enabled us to do a thorough search on the PES for local minima. The ion pairing energies obtained using the formula $\Delta E = E_{\text{ionpair}} - E_{\text{Li}^+} - E_{\text{TFSI}^-}$ are also displayed in the respective figures (the energies of the free cation and anion (**A1**) being -7.23554 and -1821.18781 au , respectively). The relative stabilization energies for the free anion and all the ion pair conformers (with and without including corrections due to zero-point energies), with respect to the corresponding lower energy structure, are given in Table 2. The total electronic energy for the most stable ion pair conformer, **A1a**, turns out to be -1828.65418 au .

The docked ion pairs from the **A1** conformer converge to **A1a-d** conformers in the HF optimization. In fact, the ion pair conformer **A1a** was obtained from docked geometries of both **A1** and **A2**. The HF calculated interaction energies range from -491 to -607 kJ mol^{-1} . In the optimization of docked ion pairs obtained from **A2**, the anionic backbone undergoes a large change, except for the **A2c** conformer. For example, in the coordination of Li^+ with a CP near O2 and O3 of the **A2** conformer, the CF_3SO_2 group rotates around the N-S bond in a clockwise direction yielding the **A1a** ion pair. The association of the cation with a CP related to the O1 and O3 atoms converges to **A2a** conformer with the CF_3SO_2 group rotating in the counterclockwise direction. In both of the conformers of the TFSI anion, a (3, +3) CP near the nitrogen is present. Optimizations of the docked geometries from the **A1** and **A2** conformers corresponding to this CP converge to ion pairs **A1b** and **A2b**, respectively. Thus, the binding of Li^+ with the TFSI anion (**A2**) leads to a large twisting around the SNS "hinge". Relatively less conformational relaxation of the anionic back-

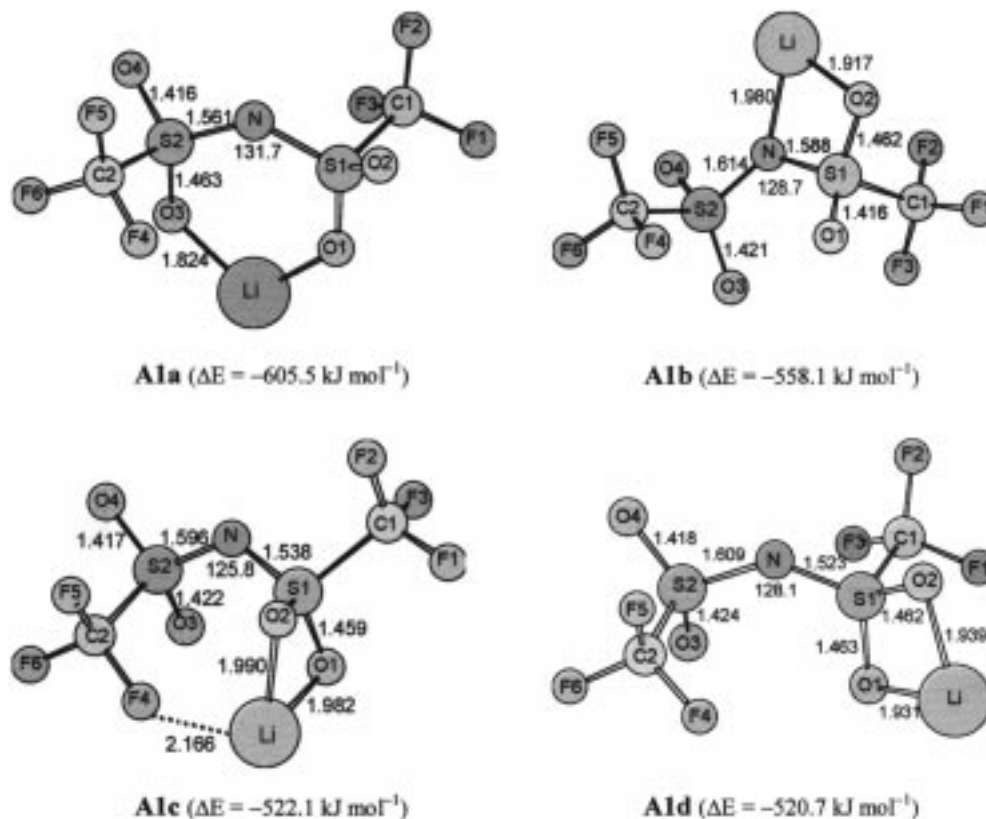


Figure 3. Geometries of ion pairs having the backbone resembling an anion with C_2 symmetry.

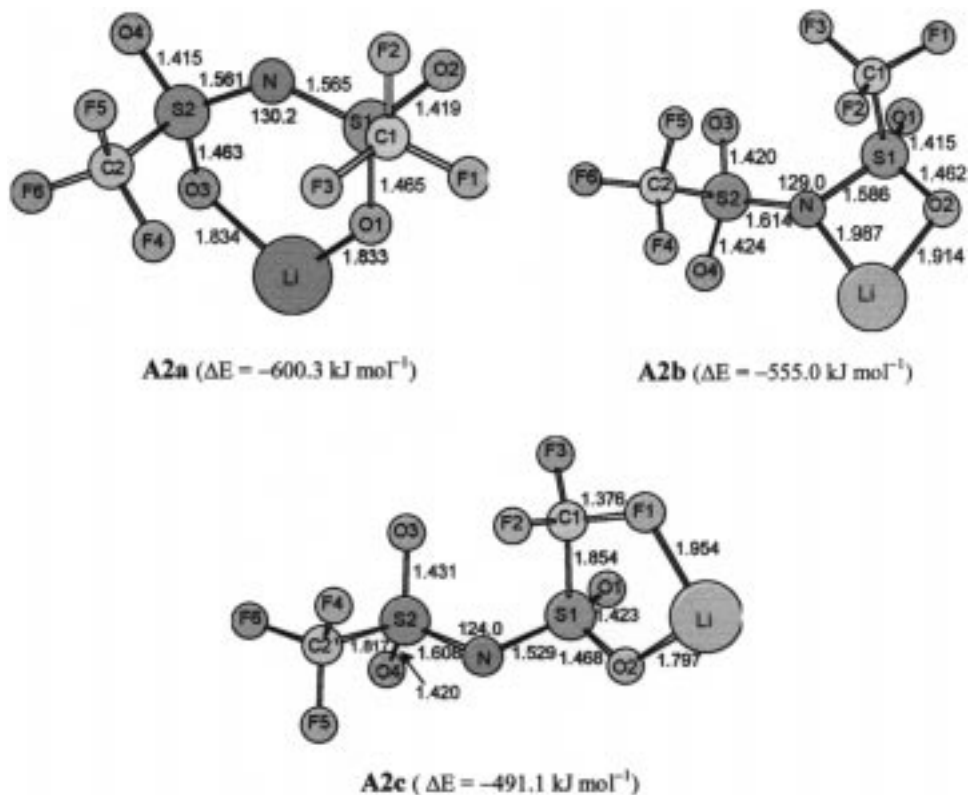


Figure 4. Geometries of ion pairs having the backbone resembling an anion with C_1 symmetry.

bone is expected in any of the optimized geometries obtained from the **A1** docked ion pairs.

Selected HF/6-31G(d) optimized geometry parameters for the **A1a-d** and **A2a-c** ion pairs are also presented in Figures 3 and 4. A comparison of the geometrical parameters of the most stable ion pair conformer (**A1a**) generally agrees well with the

experimental geometrical parameters of the HTFSI¹¹ and LiTFSI.²⁷ It is also noted that the HF/6-31G(d) optimized SNS bond angle in these ion pair conformers ranges from 124° to 132°, as compared to 142° to 172° obtained from the 3-21+G basis calculations reported by Arnaud et al.¹⁰ The CS1S2C' twist angle for the **A1a-d** and **A2a-c** are 162.6°, 183.4°, 154.4°,

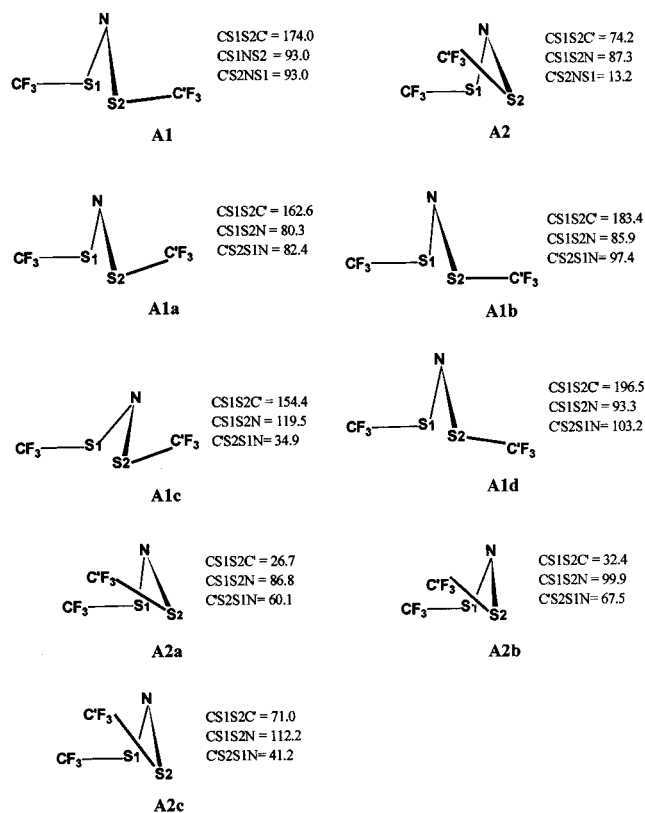


Figure 5. Schematic diagrams showing the twist (in degrees) around the SNS "hinge" in the free TFSI anion (**A1** and **A2**) and the ion pairs (**A1a–d** and **A2a–c**). For clarity, oxygen and lithium coordination are not shown here. See Figures 3 and 4 as well as the text for more details.

TABLE 2: Relative Energies with and without Including Corrections Due to Zero-Point Energies (in kJ mol⁻¹) of the TFSI Anion and the Li⁺TFSI⁻ Conformers (See Text for Details)

	A1	A2	A1a	A1b	A1c	A1d	A2a	A2b	A2c
ΔE (uncorr.)	0.00	2.28	0.00	47.44	83.86	84.88	5.19	50.53	114.41
ΔE (corr.)	0.00	1.96	0.00	46.47	81.22	82.98	5.17	49.62	112.25

196.5°, 26.7°, 32.4°, and 71.0°, respectively, as compared to those of **A1** (174.0°) and **A2** (74.2°). A schematic representation of the free anion and the ion pairs depicting these angles as well as CS1S2N and C'S2S1N are depicted in Figure 5. The following inferences may be drawn from this figure. The S1NS2 plane is nearly perpendicular to either CS1S2 or C'S2S1 planes in all the ion pairs as well as free anionic conformers. The absence of an ion pair structure having a CS1S2C' twist beyond 197° indicates that the CF₃ rotations around the SN bonds are restricted to the SNS side of the anionic backbone. In fact, this could be the reason we have not observed a structure corresponding to the lithium cation in coordination with two fluorine atoms of different CF₃ groups. Such a structure was reported by Arnaud and co-workers¹⁰ with the HF/3-21G+ level of theory.

It is noteworthy that even though the anion prefers a C₂ symmetry conformation in the free state as well as in the ion pair as in **A1a**, the energetically closer **A2** conformer renders additional possibilities for coordination of the cation with a more flexible anionic backbone. The ion pairs can be classified as conformers **A1a** and **A2a**, where the cation coordinating to two oxygen atoms of the different SO₂ groups, **A1b** and **A2b**, where the cation is in coordination with the nitrogen and oxygen, **A1c** and **A1d**, where the Li⁺ is coordinating with two oxygen atoms

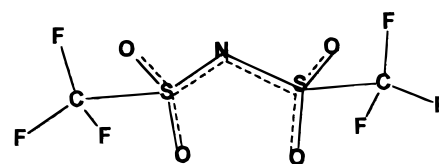


Figure 6. Stick model of TFSI anion. The dotted lines represent the excess electron distribution over the S–O and N–S bonds. See the text, Table 1, and Figure 2 for more details.

of the same SO₂ group, and **A2c**, having Li⁺ in coordination with one oxygen and one fluorine atom. Thus, the electrostatic topography assisted ab initio optimization seems to offer valuable insights for systematically probing the potential energy surface of the Li⁺TFSI⁻ ion pair.

A general observation is that whenever lithium coordinates with an oxygen (structures **A1a**, **A1c**, **A1d**, **A2a**, and **A2c**), the corresponding S–O bond is elongated by ~0.03 Å and the immediate S–N bond is shortened by 0.01–0.05 Å, as compared to the corresponding values in the free anion. In the case of **A1b** and **A2b**, lithium has a coordination with nitrogen atom and this leads to the elongation of the N–S bonds. This can be rationalized in the following manner. As we have seen, the MESP picture of the TFSI anion shows that the most negative valued regions are around the oxygen and the nitrogen atoms. In fact, it can be noticed that in the free anion the oxygen and the nitrogen atoms are connected to one and two atoms, respectively, one short of their natural valency, leading to excess π -electrons in this regions. The situation can be best described as in Figure 6. The coordination of Li⁺, for example, to two oxygen atoms changes this scenario. The coordinated atoms achieve the valency of two, and as a result the other S–O and the S–N bonding becomes tighter. On the other hand, an Li–N coordination (**A1b** and **A2b**) helps the nitrogen to get its natural valency of three that leads to the elongation of the N–S bonds and the shortening of the S–O bonds.

c. Vibrational Analysis. To initialize the understanding of the ionic association and the nature of charge carriers in the solid polymer electrolytes, the assignment to the normal vibrations of the free Li⁺TFSI⁻ ion pair were carried out. Rey et al.¹³ have analyzed the vibrational spectra of the free TFSI anion with the C₂ symmetry (**A1** conformer). The vibrational frequencies of both conformers of the free anion and the Li⁺TFSI⁻ ion pairs are reported in Table 3. The experimental data are not provided, as they are not available for this ion pair. The vibrational frequency assignments have been based on the calculations of potential energy distributions (PED) derived from the method approach proposed by Gwinn.²⁸ Assignments carried out in this way have also been presented earlier for the CF₃SO₃⁻ and related systems in the literature.²⁹ This proposed assignments in the present work generally agree well with the recent reports by Rey et al.¹³ for the HTFSI molecule. The vibrations below 300 cm⁻¹ are strongly coupled with different torsional modes, and therefore, it is generally difficult to assign these normal vibrations.

O–Li Vibrations. The relatively intense S–O–Li bending vibrations coupled with different bending coordinates occur at 534 cm⁻¹ in the oxygen-coordinating structures and at 556 cm⁻¹ when the F atom is coordinating with the cation, as in the **A2c** conformer. The Li⁺–O stretching vibrations in different conformers range from 614 cm⁻¹ (in **A1a**) to 622 cm⁻¹ (in **A2c**). These vibrational frequencies are not in accordance with the trend exhibited by the O–Li bond length parameters in different ion pair geometries. For example, the O–Li bond length increases from 1.824 Å (in **A1a**) to 1.931 Å (in **A1d**). The

TABLE 3: Vibrational Frequencies (in cm⁻¹) of the Free TFSI Anion and the Li⁺TFSI⁻ Conformers^a

assignment	TFSI ⁻		Li ⁺ TFSI ⁻						
	A1	A2	A1a	A1b	A1c	A1d	A2a	A2b	A2c
SN tors + CS tors	34	20	14	22	38	29	28	29	26
SN tors + CS tors	50	42	22	47	49	39	38	44	27
	53	55	56	53	71	49	57	59	55
	59	80	65	69	98	59	70	75	82
CF ₃ tors	125	110	111	118	113	107	119	120	95
	176	177	121	125	130	136	140	125	108
CF ₃ rock	220	190	216	144	155	147	194	161	185
	227	221	233	223	198	206	212	219	199
	252	227	237	232	222	221	234	226	222
	306	306	245	253	235	259	260	241	249
CF ₃ rock	320	319	312	293	281	296	312	293	276
	345	335	318	307	313	310	316	309	312
SO ₂ rock	361	366	343	324	319	344	326	314	330
	376	370	367	364	329	353	365	365	362
SO ₂ twist	399	391	371	366	364	362	371	367	366
SO ₂ wag	432	444	380	390	368	372	383	388	378
SO ₂ wag	448	525	415	411	397	396	430	401	398
CF ₃ bend	564	555	458	442	447	433	458	445	431
	584	575	489	451	490	467	491	467	461
LiO*S bend			534	531	520	556	548	536	556
SO ₂ bend	601	599	592	577	564	572	589	575	573
SO ₂ bend	610	615	593	582	590	595	593	584	590
CF ₃ bend	631	621	609	606	599	601	609	606	609
OLi str			614	612	612	611	616	613	622
SO ₂ bend	655	632	661	642	627	635	642	640	627
			683	653	663	676	669	657	637
SNS bend	703	681	702	707	680	695	691	675	708
	703	752	718	730	742	711	741	751	738
SN str	815	815	816	835	815	818	816	833	810
CF ₃ bend	852	852	862	862	851	862	861	860	850
CS str	873	873	886	893	884	885	890	888	879
SO ₂ str + SN str	1179	1175	1157	1160	1155	1149	1149	1158	1128
SO ₂ str + SN str	1257	1253	1220	1206	1208	1254	1218	1213	1205
SO ₂ str	1272	1269	1261	1260	1272	1281	1252	1261	1244
CF ₃ str	1379	1374	1389	1376	1290	1296	1385	1380	1275
CF ₃ str	1381	1379	1400	1385	1295	1381	1396	1393	1400
CF ₃ str	1388	1388	1404	1408	1384	1395	1401	1405	1409
CF ₃ str	1394	1394	1405	1412	1428	1415	1417	1413	1416
CF ₃ str	1416	1417	1437	1431	1435	1423	1436	1427	1428
CF ₃ str	1417	1422	1445	1446	1450	1432	1439	1439	1431
SO ₂ str	1444	1444	1455	1470	1453	1445	1448	1470	1484
SO ₂ str	1473	1459	1474	1511	1511	1506	1472	1509	1491

^a Rock = rocking, tors = torsion, twist = twisting, wag = wagging, bend = bending, str = stretching. Atoms with * denote directly bonded atoms.

stretching frequencies, however, show a little variation in these conformers. In the **A2c** conformer, where the O–Li distance (1.791 Å) is much shorter than that in **A1a**, this vibration is predicted to be 8 cm⁻¹ higher, as expected. These stretching vibrations involve a strong coupling with the different bending coordinates.

S–N Vibrations. The shortening of the S–N bonds in the ion pair conformers is not manifested in the stretching vibrational frequencies since these are largely mixed. The S–N stretching vibrational frequencies of the TFSI anion in the electrolytes containing PEO and LiTFSI are observed⁸ at 767 and 742 cm⁻¹. The SNS bending vibrations are strongly coupled with the N–S–O bendings. SNS deformations at 655 cm⁻¹ observed in the polymer electrolytes are predicted to be 703 (doublet) and 681 cm⁻¹ for the **A1** and **A2** conformers of the free anion, respectively. The 683 cm⁻¹ vibration is nearly unchanged in the **A1a** ion pair from the present HF/6-31G(d) calculations. In the remaining ion pair conformers, this vibration is predicted to be in the range 675–708 cm⁻¹. Both the **A1**

and **A2** conformers exhibit an intense band near 815 cm⁻¹ which is assigned to the S–N stretching. The low-lying **A1a** and **A2a** conformers show nearly no shift for this characteristic vibration (compared to **A1**), whereas the nitrogen-coordinating ion-pairs exhibit a frequency upshift of 18–20 cm⁻¹. This vibration was used as a probe to identify the possible different cation-coordinating geometries of the M⁺–TFSI⁻ ion pairs. The HF/6-31G(d) calculated bands at 815, 852, and 874 cm⁻¹ in both the **A1** and **A2** conformers may be identified easily in the observed spectra since they are isolated from neighboring bands on both sides by more than 60 cm⁻¹. The experimental band positions, however, are found to be about 80 cm⁻¹ lower than the calculated ones (such a difference is expected for the HF frequencies) The lowest wavenumber vibration of this, having a substantial S–N stretching contribution, was selected for a detailed study of the measured spectra of the electrolytes containing alkaline earth metal (M) cations, as in M(CF₃SO₂)₂-NP(EO)_n. The infrared bands appear at 746, 747, and 748 cm⁻¹ for Ba²⁺, Sr²⁺, and Ca²⁺, respectively, and 743 cm⁻¹ for Mg²⁺. The observed band at 740 cm⁻¹ is attributed to the free imide anions. The observed perturbations of the S–N stretching modes are probably due to anions paired with the cations. For M = Ca, Sr, Ba in the M²⁺TFSI⁻ ion pairs complexed with PEO, the shift of the ion pair component increases with the decreasing size of the cation. This is expected, since the Coulomb attraction of the metal cation of smaller size causes a large perturbation of the anion vibrational mode. However, the relatively small shift for the Mg²⁺ may be attributed to a different type of coordination than the samples containing the large cations. Thus, the formation of an ion pair with the cation coordinating with the two oxygens from two different SO₂ groups was proposed for Mg²⁺ by Lindgren et al.⁷ For the remaining cations, a nitrogen-coordinating ion pair structure was suggested. It should, however, be noted that the FTIR measurements of the solvated TFSI anion show bands at 1056 and 766 cm⁻¹ which were assigned to the S–N stretching by Rey and co-workers.¹³ These may be correlated with the 1179 and 815 cm⁻¹ vibration in the **A1** conformer of the free anion in the present calculations. The 815 cm⁻¹ vibration remains unchanged in both the conformers of the anion. In gel electrolytes containing the LiTFSI, no contact ion pairs are formed until the concentration of 5 M is reached. At this stage, however, the substantial ionic association occurs. The ion pairing in this case can be monitored by the infrared bands of the TFSI anion in the region 730–820 cm⁻¹.

SO₂ Vibrations. Rey et al.⁹ have pointed out that the asymmetric SO₂ stretching is expected in the region 1300–1350 cm⁻¹. In the aqueous solutions of the TFSI, the infrared bands at 1334 and 1350 cm⁻¹ are observed. These SO₂ stretchings can be correlated with the intense vibrations at 1444 and 1473 cm⁻¹ obtained from the HF/6-31G(d) calculations for the **A1** conformer. Thus, the predicted separation of these SO₂ stretching vibrations is nearly twice as large than the observed one. The higher wavenumber vibration of these two is nearly unchanged in the two low-energy conformers (**A1a**, **A2a**) of the Li⁺TFSI⁻ ion pair. The nitrogen-coordinating structures (**A1b** and **A2b**) of the ion pairs, however, show a frequency upshift of 40 cm⁻¹ in this case. In the **A2** conformer of the anion, these are almost purely localized in each SO₂ group at 1444 and 1459 cm⁻¹, respectively. The relatively simple vibrational behavior is destroyed in the ion pairs. The internal S–O coordinates become mixed and, in addition, some C–F contributions were noted for these normal modes. Our earlier calculations on the simpler triflate ion (CF₃SO₃)⁻ have revealed that the prediction of the relative order of the S–O and C–F

stretching bands at the HF level was difficult.³⁰ All this makes the S–O stretching vibrations less suitable than the S–N stretchings for a prediction of the coordinating geometries in an experimental situation. The normal vibrations in the range 1128 to 1281 cm⁻¹ of the free ion as well as those in the ion pair conformers assigned to the SO₂ bending vibrations have a significant contribution from the S–N modes.

CF₃ Vibrations. Wen et al.⁸ have assigned the 1207 and 1143 cm⁻¹ vibrations as the CF₃ stretchings. The symmetric stretching occurs at a higher wavenumber than the asymmetric one in the PEO–LiTFSI electrolytes. From the present calculations, this band can be correlated with a band at 1405–1417 cm⁻¹ vibration in the Li⁺TFSI⁻ ion pair. The CF₃ stretching vibrations of the free anion conformers in the 1379–1394 cm⁻¹ region are relatively pure. A near doublet found at 1416 cm⁻¹ in the free TFSI anion (A1 conformer) splits by about 5 cm⁻¹ in the A2 conformer of the free anion. Splitting as large as 10–15 cm⁻¹ for the same was predicted in some of the ion pair conformers. These vibrations are strongly coupled with the C–S and S–N vibrations. The CF₃ asymmetric bendings in the 430–490 cm⁻¹ region are perturbed largely in the Li⁺TFSI⁻ conformers.

Concluding Remarks

The structures of the Li⁺TFSI⁻ ion pair conformers have been predicted with the HF/6-31G(d) theory using the topography of the molecular electrostatic potential of the anion as a tool. It has been demonstrated that the MESP topography provides a systematic way to analyze the formation of different ion pair conformers. The calculations predict that the interaction of the (CF₃SO₂)₂N⁻ occurs prominently via the oxygen atoms of the SO₂ groups of the anion conformers, which may well be seen through the MESP minima exhibited by these atoms. The nitrogen-coordinating Li⁺TFSI⁻ conformers are nearly 50 kJ mol⁻¹ higher in energy than the minimum energy structure. The SNS bond angle in the free anion and the Li⁺TFSI⁻ ion pair systems ranges from 126°–132°, in good agreement with that derived from the diffraction experiments on similar ions or molecules. HF/6-31G(d) vibrational frequencies of the Li⁺TFSI⁻ conformers show that the S–N stretching vibration near 815 cm⁻¹ can be used as a probe to distinguish the ion pair conformers. Thus, the present work may represent a first step in the interpretation of the experimental vibrational spectra of the polymer electrolytes M⁺–TFSI⁻P(EO)_n.

Acknowledgment. S.P.G. acknowledges the support from the University Grants Commission [Project 12-37/97 (SR-I)], New Delhi, India and the Jawaharlal Nehru Center for Advanced Scientific Research, Bangalore, India for providing a visiting fellowship during which a part of these computations were carried out. Thanks are due to Professor J. Chandrashekar for valuable discussions. Authors C.H.S., K.B., and S.R.G. are thankful to the Council of Scientific and Industrial Research (CSIR), India [01(1430)/EMR-II/96].

References and Notes

(1) Armand, M.; Gorecki, W.; Andreani, R. In *2nd International Symposium on Polymer Electrolytes*; Scrosati, B., Ed.; Elsevier: London, 1990; p 91.

- (2) Sylla, S.; Sanchez, J. Y.; Armand, M. *Electrochim. Acta* **1992**, *37*, 1699.
- (3) Andreev, Y. G.; Lightfoot, P.; Bruce, P. G. *J. Chem. Soc., Chem. Commun.* **1996**, 2170.
- (4) Brown, S. D.; Grienbaum, S. G.; McLin, M. G.; Wintersgill, M. C.; Fontanella, J. J. *Solid State Ionics* **1994**, *67*, 257.
- (5) Vallee, A.; Besner, S.; Prudhomme, J. *Electrochim. Acta* **1992**, *37*, 1579.
- (6) Johansson, A.; Gogll, A.; Tegenfeldt, J. *Polymer* **1996**, *37*, 1387.
- (7) Bakker, A.; Gejji, S. P.; Lindgren, J.; Hermansson, K.; Probst, M. *Polymer* **1995**, *36*, 4371.
- (8) Wen, S. J.; Richardson, T. J.; Ghantous, D. I.; Stribel, K. A.; Ross, P. N.; Cairns, E. J. *J. Electroanal. Chem.* **1996**, *408*, 113; **1996**, *415*, 197.
- (9) Rey, I.; Lassegues, J. C.; Grondin, J.; Servant, L. *Electrochim. Acta* **1998**, *43*, 1505.
- (10) Arnaud, R.; Benrabah, D.; Sanchez, J. Y. *J. Phys. Chem.* **1996**, *100*, 10882.
- (11) Hass, A.; Klare, Ch.; Betz, P.; Bruckmann, J.; Kruger, C.; Tsay Y.-H.; Aubke, F. *Inorg. Chem.* **1996**, *35*, 1918.
- (12) Johansson, P.; Gejji, S. P.; Tegenfeldt, J.; Lindgren, J. *Electrochim. Acta* **1998**, *43*, 1375.
- (13) Rey, I.; Johansson, P.; Lindgren, J.; Lassegues, J. C.; Grondin, J.; Servant, L. *J. Phys. Chem. A* **1998**, *102*, 3249.
- (14) Gadre, S. R.; Bhadane, P. K.; Pundlik, S. S.; Pingale, S. S. In *Molecular Electrostatic Potentials: Concepts and Applications*; Murray, J. A., Sen, K., Eds.; Elsevier: Amsterdam, 1996; Chapter 5, p 219.
- (15) (a) Gadre, S. R.; Shrivastava, I. H. *J. Chem. Phys.* **1991**, *94*, 4384. (b) Gadre, S. R.; Kulkarni, S. A.; Shrivastava, I. H. *J. Chem. Phys.* **1992**, *96*, 5253.
- (16) See, for example: (a) Legon, A. C.; Millen, D. J. **1987**, *16*, 467. (b) Dykstra, C. E. *J. Am. Chem. Soc.* **1989**, *111*, 6168. (c) Alhabama, C.; Luque, F. J.; Orozco, M. *J. Phys. Chem.* **1995**, *99*, 3084.
- (17) Buckingham, A. D.; Fowler, P. W. *J. Chem. Phys.* **1983**, *79*, 6426. Buckingham, A. D.; Fowler, P. W. *Can. J. Chem.* **1985**, *63*, 2018.
- (18) Politzer, P.; Trulhar, D. G., Eds. *Chemical Applications of Atomic and Molecular Electrostatic Potentials*; Plenum: New York, 1981.
- (19) Náráy-Szabó, G.; Ferenczy, G. C. *Chem. Rev.* **1995**, *4*, 829.
- (20) Bonnacorsi, R.; Scrocco, E.; Tomasi, J. *J. Chem. Phys.* **1970**, *52*, 5270. Bonnacorsi, R.; Scrocco, E.; Tomasi, J. *Theor. Chim Acta* **1979**, *52*, 13. Tomasi, J.; Bonnacorsi, R.; Cammi R. In *Theoretical Models of Chemical Bonding*, Vol. 4; Maksić, Z. B., Ed.; Springer: Berlin, Heidelberg, New York, 1991; p 228.
- (21) Gejji, S. P.; Suresh, C. H.; Bartolotti L. J.; Gadre, S. R. *J. Phys. Chem. A* **1997**, *101*, 5678.
- (22) Suresh, C. H.; Gadre, S. R.; Gejji, S. P. *Theor. Chem. Acc.* **1998**, *99*, 151.
- (23) Frisch, M. J.; Trucks, G. W.; Schlegel, H. B.; Gill, P. M. W.; Johnson, B. G.; Robb, M. A.; Cheeseman, J. R.; Keith, T. A.; Peterson, G. A.; Montgomery, J. A.; Raghavachari, K.; Al-Laham, M. A.; Zakrzewski, V. G.; Ortiz, J. V.; Foresman, J. B.; Cioslowski, J.; Stetanov, B. B.; Nanayakkara, A.; Challacombe, M.; Peng, C. Y.; Ayala, P. Y.; Chen, W.; Wong, M. W.; Andres, J. L.; Replogle, E. S.; Gomperts, R.; Martin, R. L.; Fox, D. J.; Binkley, J. S.; DeFrees, D. J.; Baker, J.; Stewart, J. P.; Head Gordon, M.; Gonzalez C.; Pople, J. A. *GAUSSIAN 94*, revision E.2; Gaussian: Pittsburgh, PA, 1995.
- (24) Fortran code UNIPROP developed by S. R. Gadre and others. For UNIVIS (a PC based molecular property visualization package), see: Limaye, A. C.; Inamdar, P. V.; Dattawadkar, S. M.; Gadre, S. R. *J. Mol. Graphics* **1996**, *14*, 19.
- (25) Williams, D. E.; Yan, J. M. *Adv. At. Mol. Phys.* **1988**, *23*, 87.
- (26) Chipot, C.; Angyan, J. G. *GRID-3.0*, a Fortran code performing charge fitting to molecular electrostatic potentials of fields, 1992.
- (27) Nowinski, J. L.; Lightfoot, P.; Bruce, P. G. *Mater. Chem.* **1994**, *4*, 1579.
- (28) Gwinn, W. D. *J. Chem. Phys.* **1971**, *55*, 477.
- (29) Gejji, S. P.; Hermansson, K.; Lindgren, J. *J. Phys. Chem.* **1993**, *97*, 6986. Gejji, S. P.; Hermansson, K.; Tegenfeldt, J.; Lindgren, J. *J. Phys. Chem.* **1993**, *97*, 11402. Gejji, S. P.; Hermansson, K.; Lindgren, J. *J. Phys. Chem.* **1994**, *98*, 8687.
- (30) Gejji, S. P.; Hermansson, K.; Lindgren, J. *J. Phys. Chem.* **1993**, *97*, 3712.